Mutagenesis Evidence that the Partial Reactions of Firefly Bioluminescence Are Catalyzed by Different Conformations of the Luciferase C-Terminal Domain†

Bruce R. Branchini,* Tara L. Southworth, Martha H. Murtiashaw, Sara R. Wilkinson, Neelum F. Khattak, Justin C. Rosenberg, and Marc Zimmer

Department of Chemistry, Connecticut College, New London, Connecticut 06320

Received September 27, 2004; Revised Manuscript Received November 11, 2004

ABSTRACT: Firefly luciferase catalyzes two sequential partial reactions resulting in the emission of light. The enzyme first catalyzes the adenylation of substrate luciferin with Mg-ATP followed by the multistep oxidation of the adenylate to form the light emitter oxyluciferin in an electronically excited state. The beetle luciferases are members of a large superfamily, mainly comprised of nonbioluminescent enzymes that activate carboxylic acid substrates to form acyl-adenylate intermediates. Recently, the crystal structure of a member of this adenylate-forming family, acetyl-coenzyme A (CoA) synthetase, was determined in complex with an unreactive analogue of its acyl-adenylate and CoA [Gulick, A. M., Starai, V. J., Horswill, A. R., Homick, K. M., and Escalante-Semerena, J. C. (2003) *Biochemistry 42*, 2866−2873]. This structure presented a new conformation for this enzyme family, in which a significant rotation of the C-terminal domain brings residues of a conserved β-hairpin motif to interact with the active site. We have undertaken a mutagenesis approach to study the roles of key residues of the equivalent β-hairpin motif in *Photinus pyralis* luciferase (^{442}IleLysTyrLysGlyTyrGlnVal^{449}) in the overall production of light and the individual adenylation and oxidation partial reactions. Our results strongly suggest that Lys443 is critical for efficient catalysis of the oxidative half-reaction. Additionally, we provide evidence that Lys443 and Lys529, located on opposite sides of the C-terminal domain and conserved in all firefly luciferases, are each essential for only one of the partial reactions of firefly bioluminescence, supporting the proposal that the superfamily enzymes may adopt two different conformations to catalyze the two half-reactions.

Light emission by the North American firefly *Photinus pyralis* is a familiar example of bioluminescence, the conversion of chemical energy into light by a living organism. Firefly bioluminescence is catalyzed (*1*−*6*) by the enzyme luciferase (Luc).[1] The beetle luciferases (*3*, *7*−*14*), including Luc, are members of the "acyl-adenylate/thioester-forming" superfamily of enzymes (*15*−*17*) that also includes a variety of acyl:CoA ligases that activate acetate and fatty acids of various lengths (*18*). Other CoA ligases produce adenylates from hydroxy- and chlorobenzoates, cinnamate, malonate, and other organic acids (*15*−*17*, *19*, *20*). The superfamily also contains the acyl-adenylate-forming domains of enzyme complexes involved in the nonribosomal synthesis of peptides and polyketides (NRPSs) (*21*−*25*). All of these enzymes catalyze two partial reactions (Figure 1). In the first reaction, an acyl-adenylate intermediate is formed from a carboxylic acid substrate and ATP. Using this common chemistry, luciferase produces enzyme-bound LH_2-AMP (eq 1) from substrates luciferin (LH_2) and Mg-ATP.

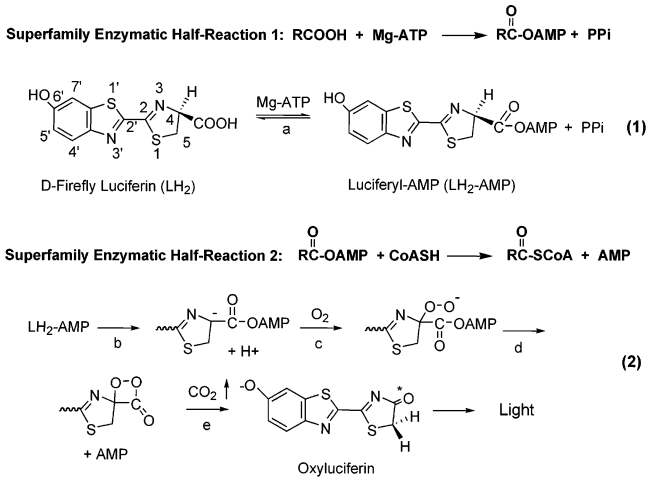

FIGURE 1: Partial reactions of the acyl-adenylate-forming superfamily of enzymes and mechanism of adenylation and oxidation steps in firefly bioluminescence.

† This work was supported by Grants from the National Science Foundation (MCB 9816898 and MCB 0130908) and the Hans and Ella McCollum '21 Vahlteich Endowment.

* To whom correspondence should be addressed: Department of Chemistry, Connecticut College, 270 Mohegan Avenue, New London, CT 06320. Telephone: (860) 439-2479. Fax: (860) 439-2477. E-mail: brbra@conncoll.edu.

[1] Abbreviations: bAcs, acetyl-CoA synthetase from *Salmonella enterica*; yAcs, acetyl-CoA synthetase from yeast; At4CL2, 4-coumarate:coenzyme A ligase from *Arabidopsis thaliana*; CBA, 50 mM Tris-HCl at pH 7.0 containing 150 mM NaCl, 1 mM EDTA, 1 mM DTT, 0.8 M ammonium sulfate, and 2% glycerol; CoA, coenzyme A; DHB, 2′,3′-dihydroxybenzoate; DhbE, 2′,3′-dihydroxybenzoate adenylation domain for bacillibactin synthesis in *Bacillus subtilis*; GST, glutathione-*S*-transferase; L, dehydroluciferin; L-AMP, dehydroluciferyl-*O*-adenosine monophosphate; LH_2, D-firefly luciferin; LH_2-AMP, D-luciferyl-*O*-adenosine monophosphate; Luc, *Photinus pyralis* luciferase (E.C. 1.13.12.7); NRPS, nonribosomal peptide synthetase; PheA, phenylalanine-activating subunit of gramicidin synthetase 1; Ppy WT, recombinant *Photinus pyralis* luciferase containing the additional N-terminal peptide GlyProLeuGlySer.

10.1021/bi047903f CCC: $30.25
Published on Web 01/08/2005

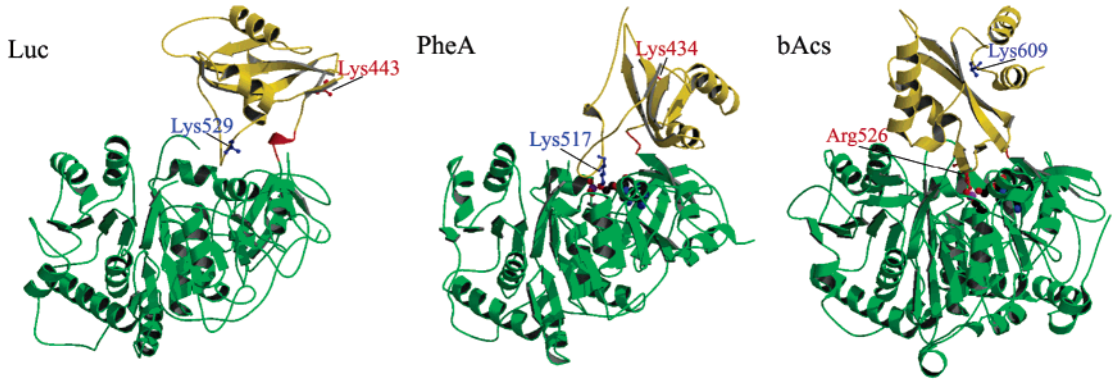

FIGURE 2: Comparison of the conformations of the Luc, PheA, and bAcs X-ray structures. In each figure, the secondary structures of the N domain (green), C domain (yellow) and hinge regions (orange) are shown. The stringently conserved Lys residues equivalent to Lys529 in Luc are shown in blue, and basic A8 β-hairpin residues similar to Lys443 are indicated in red. The active sites of PheA and bAcs contain Phe plus AMP and inhibitor adenosine-5′-propylphosphate, respectively. This figure was produced with MolScript (*54*), BobScript (*55*), POVScript+ (*56*), and Raster3D (*57*).

Many of the superfamily enzymes generate CoA thioester intermediates or products from the initially formed adenylates (Figure 1), while the NRPS domains transfer the acyl substrate to the thiol group of protein-bound cofactor 4′-phosphopantetheine (*23*). In its second partial reaction, the luciferases differ from other superfamily enzymes in that they function as monooxygenases in the multistep conversion of LH_2-AMP into oxyluciferin and light (eq 2). In the generally accepted mechanism (*1*−*6*), Luc first catalyzes the addition of molecular oxygen to a presumed C-4 anionic intermediate of LH_2-AMP likely leading to the formation of a highly reactive dioxetanone species. Release of carbon dioxide accompanies the formation of excited-state oxyluciferin, the light-emitting product. While CoA is not required for bioluminescence, the cofactor does have a stimulatory effect on light production (*26*−*28*).

Studies of Luc function (*29*−*33*) have been advanced with the availability of the Luc X-ray crystal structure data (*34*, *35*), although the structures do not contain bound substrates. The Luc crystal structures and those of four nonbioluminescent superfamily enzymes (*36*−*39*) share a unique protein fold that consists of a large N-terminal domain (residues 1−436 in Luc) linked to a smaller C-terminal domain (residues 440−550) through a short putative hinge (residues 437−439). The Luc structure represents an open conformation in which the domains are well-separated (Figure 2). The closed conformations of DhbE, the 2′,3′-dihydroxybenzoate adenylation domain of *Bacillus subtilis*, with bound adenylate DHB-AMP (*37*) and the yeast acetyl-CoA synthetase (yAcs) in a binary complex with AMP (*39*) are very similar to the phenylalanine-activating subunit of gramicidin synthetase 1 (PheA) in complex with phenylalanine, Mg ion, and AMP (*36*). In PheA, the C-terminal domain is rotated 94° and is ∼5 Å closer to the N-terminal domain than in the Luc structure (Figure 2). A rotated conformation was seen in the structure of bacterial acetyl-CoA synthetase (bAcs) complexed with adenosine-5′-propylphosphate, an unreactive analogue of the acyl-adenylate, and CoA (*38*). The C-terminal domain of bAcs is rotated ∼140° relative to the conformation of PheA, DhbE, and yAcs (Figure 2). The crystallography results prompted Gulick et al. (*38*) to propose that the superfamily enzymes may adopt two different conformations to catalyze the two half-reactions, adenylation in the PheA closed conformation and thioester formation in the bAcs rotated form. This sound proposal awaits confirmation by crystallization of the same enzyme in both orientations.

On the basis of an analysis of sequence alignments of NRPSs, 10 conserved regions of the superfamily have been identified (*40*) including two, A8 and A10, which are on opposite sides of the C-terminal domains. The crystal structures of the enzymes in the PheA conformation contain a stringently conserved lysine (Lys529 in Luc) of A10 at their active sites. Our prior mutagenesis studies (*31*) of Lys529 in Luc suggested that this residue is critical for effective substrate orientation and that it provides favorable polar interactions important for transition-state stabilization leading to efficient adenylate production (eq 1). In contrast, the residues ^{523}SerGlyHisArg^{526} of the conserved β-hairpin motif of A8 in the bAcs structure make interactions with N-domain residues, the adenylate analogue, and CoA, while the A10 domain is ∼30 Å away (Figure 2). Possibly, the formation and oxidation of LH_2-AMP requires rotation of the Luc C-terminal domain into conformations similar to those revealed by the structures of PheA and bAcs. To address this possibility, we have undertaken a mutagenesis approach to study the roles of key residues of the Luc β-hairpin motif (^{442}IleLysTyrLysGlyTyrGlnVal^{449}) in the overall production of light and the individual adenylation and oxidation partial reactions.

MATERIALS AND METHODS

Materials. The following items were obtained from the indicated sources: Mg-ATP (bacterial), CoA sodium salt (Sigma), LH_2 (Biosynth AG), restriction endonucleases (New England Biolabs), and mutagenic oligonucleotides (Invitrogen). Ppy wild type (Ppy WT) and K529A in the pGex-6p-2 plasmid were prepared as previously reported (*29*, *31*).

General Methods. Light measurements were made in 8 × 50 mm polypropylene tubes (Evergreen Scientific, Los Angeles, CA) placed in the sample compartment of either an Aminco Chem Glow II or a Turner TD-20e luminometer. Data were acquired from the analogue output of the luminometer with a Strawberry Tree Inc. (STI) A/D converter (with a sampling rate of 0.05−0.1 s) and stored to a Macintosh computer. Light measurements were quantified with customized versions of the STI Workbench software.

All measurements were corrected for the spectral response of the Hamamatsu 931B photomultiplier tube.

All luciferases in pGex-6p-2 plasmids were expressed in *Escherichia coli* strain BL21 at 22 °C and purified by the method previously reported (*41*). Mass spectral analyses of the proteins were performed by tandem HPLC−electrospray ionization mass spectrometry using either a Perkin−Elmer Series 200 HPLC system and a Sciex ABI150A mass spectrometer or a ThermoFinnigan Surveyor HPLC system and a ThermoFinnigan LCQ Advantage mass spectrometer. The calculated molecular masses (in Daltons) of the luciferases are Ppy WT, 61 157; K443A, 61 100; K445Q, 61 157; G446I, 61 213; Q448A, 61 100; K529A, 61 100; and K443A/K529A, 61 043. The determined mass values were all within the allowable experimental error of the calculated values. The mutations of all luciferase genes were verified by DNA sequencing performed at the W. M. Keck Biotechnology Laboratory at Yale University.

Site-Directed Mutagenesis. The Quik Change Site-Directed Mutagenesis kit (Stratagene) was used to create the mutant luciferase proteins. Site-directed mutagenesis was carried out according to the instructions of the manufacturer using Ppy WT in the pGex-6p-2 vector as a template and the following primers and their respective reverse complements: K443A, 5′-CGC TTG AAG TCT TTA ATT **GCA** TAC AAA GGG TAT CAG GTG GCC-3′; K445Q, 5′-CGC TTG AAG TCT TTA ATT AAA TAC **CAA** GGG TAT CAG GTG GCC-3′; G446I, 5′-CGC TTG AAG TCT TTA ATT AAA TAC AAA **ATC** TAT CAG GTG GCC CCC-3′; and Q448A, 5′-G TCT TTA ATT AAA TAC AAA GGG TAT **GCG** GTG GCC CCC GC-3′ (bold represents the mutated codon, and underline represents silent changes to remove a unique *Eco*RV endonuclease site used for screening). The double mutant K443A/K529A was prepared using K529A in the pGex-6p-2 vector as a template and the primer set for K443A.

Steady-State Kinetic Constants. Values of K_m and V_{max} for LH_2, Mg-ATP, and LH_2-AMP for all luciferase enzymes were determined from bioluminescence activity assays in which measurements of maximal light intensities were taken, after correction for differences in rise times compared to those of Luc (0.5 s with LH_2 and Mg-ATP and 0.4 s with LH_2-AMP), as estimates of initial velocities. Data for LH_2 and Mg-ATP were collected in 0.525 mL reactions in 25 mM glycylglycine buffer at pH 7.8 containing 0.6−4.6 μg of luciferase enzyme in CBA. The concentration of one substrate was maintained at saturation, while the other was varied: 0.15−760 μM LH_2 and 6.4−7800 μM Mg-ATP. Reactions were initiated by injection of the saturating substrate. Data for LH_2-AMP were obtained in 0.510 mL reactions in 50 mM glycylglycine buffer at pH 7.8 containing 0.1 mL aliquots of LH_2-AMP solution (final concentrations of 0.025−35 μM) in 10 mM sodium acetate at pH 4.5. Immediately, light reactions were initiated by injections of 10 μL of luciferase enzymes (0.45−3.4 μg in CBA). Kinetic constants were determined using a nonlinear least-squares method of the Enzyme Kinetics Pro software (SynTex), which fits data from the Michalis−Menten equation to a rectangular hyperbola. The corresponding k_{cat} values were obtained by dividing the V_{max} values by the final amounts (in micromoles) of each luciferase in the assay mixtures. The relative rates of adenylate formation were estimated (error ± 10% of the value) by fluorescence-based assays of L-AMP formation as described previously (*31*), except that data were obtained using a Perkin−Elmer LS55 luminescence spectrometer operated in the "time-drive" mode. The value for Ppy WT determined with this instrument was 12 s^{-1}.

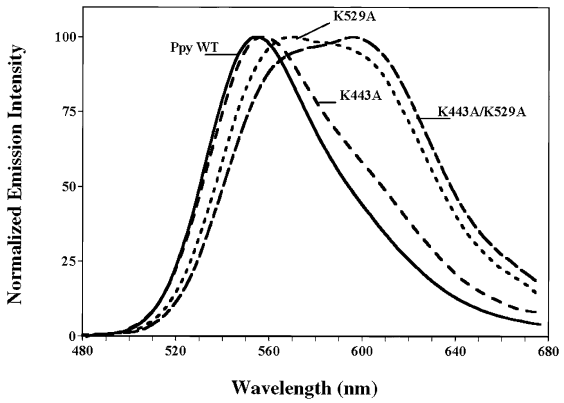

FIGURE 3: Bioluminescence emission spectra at pH 7.8. Spectra were recorded with the indicated luciferases as described under the Materials and Methods.

Bioluminescence Emission Spectra. Bioluminescence emission spectra for the luciferases with LH_2 and Mg-ATP at pH 7.8 were obtained using a Perkin−Elmer LS55 luminescence spectrometer operated in the "bioluminescence" mode. Data were collected over the wavelength range of 480−680 nm in a 1 mL optical glass cuvette. Gate and delay times, detector voltage, scan rate, and slit width were adjusted to optimize the instrument response. Data were corrected for the spectral response of the R928 photomultiplier tube using the Perkin−Elmer FL WinLab software. Bioluminescence emission spectra (Figure 3) were obtained in 0.525 mL reactions with 2 mM Mg-ATP and 70 μM luciferin in 25 mM glycylglycine buffer at pH 7.8 with final concentrations of luciferases ranging from 0.16 to 2.6 μM. The enzyme stabilizing storage reagents NaCl, ammonium sulfate, and glycerol were kept at standard concentrations of 7.2 mM, 38 mM, and 0.1%, respectively.

Effect of CoA on Total Light Yield. Estimates of the ability of CoA to sustain bioluminescence were made by measuring the total light emitted by reactions catalyzed by Ppy WT and the luciferase mutants in the presence or absence of CoA. The reactions (0.525 mL) were initiated by the injection of 0.12 mL of Mg-ATP (final concentration of 2.2 mM) into mixtures of enzymes (1.5−4.0 μg) in 25 mM glycylglycine buffer at pH 7.8 containing 70 μM LH_2 with or without 0.1 mM CoA. Relative total light emission was estimated by integration over 5 min as required to collect at least 90% of the emitted light. All measurements were performed in duplicate, and the values reported in Table 3 are expressed as ratios of the total light emitted by each enzyme in the presence of CoA divided by the value obtained in the absence of CoA.

Molecular Modeling. A combination of homology/molecular mechanics modeling was used to generate a Luc structure in the bAcs rotated conformation with bound LH_2-AMP (Figure 4). The amino acid sequence of Luc (PDB code 1BA3) was aligned with bAcs (PDB code 1PG4) using BLAST (*42*) and SSpro (*43*) to improve the alignment by taking into account secondary-structure predictions. The initial three-dimensional model of Luc in the bAcs confor-

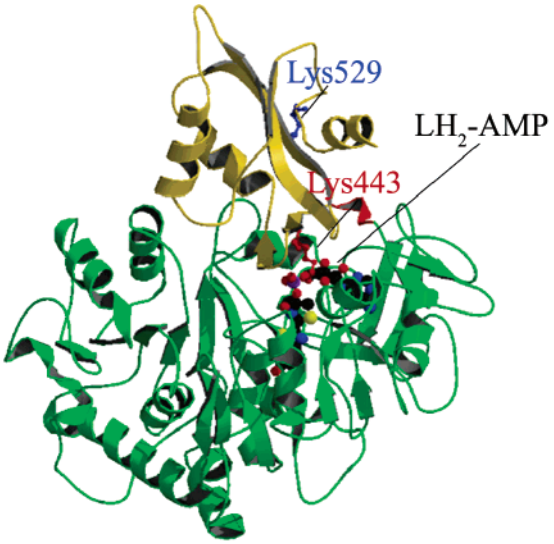

FIGURE 4: Crystal structure of Luc with LH_2-AMP modeled into the putative active site and rotated into the bAcs conformation as described in the Materials and Methods. The orientation of the Luc N-terminal domain is the same as in Figure 2. The N domain (green), C domain (yellow), hinge region (orange), Lys529 (blue), and Lys443 (red) are shown. This figure was produced with MolScript (*54*), BobScript (*55*), POVScript+ (*56*), and Raster3D (*57*).

mation was built from the resulting sequence alignment using Prime 1.0 with the OPLS_2000 all-atom force field for energy scoring, a surface-generalized Born continuum solvation model, and residue-specific side-chain rotamer and backbone dihedral libraries representing values most commonly observed in protein crystal structures. During model building, the CoA and adenosine-5′-propylphosphate ligands were kept in the active site and then removed during the subsequent active-site modeling and conformational searching. LH_2-AMP was maintained in the conformation first determined using our original active-site model (*29*) and then introduced into the newly built Luc model by superimposing the active sites of the two models. The resultant Luc·LH_2-AMP complex with the C domain rotated into the bAcs conformation was subjected to a 10 000 step Monte Carlo torsional- and molecular-position variation method conformational search (*44*, *45*) and a 10 000 step large-scale low-mode search (*46*, *47*). In the conformational searches, a hot sphere of 10 Å around LH_2-AMP was used and all atoms in this substructure were minimized without restriction. Two subsequent shells extending a further 2.00 Å each were constrained to their *x*, *y*, and *z* coordinates by a force constant of 200.00 kcal/mol Å^2 for the first shell and a force constant of 400.00 kcal/mol Å^2 for the second shell. All atoms outside the "hot" sphere and the two constrained spheres were ignored. An aqueous generalized Born continuum solvation model was used in all calculations (*48*). A total of 184 low-energy conformations were found within 20 kJ/mol of the lowest energy conformation. An examination of all of these low energy conformations found that His245, Thr343, and Lys443 were the only residues that had side chains within 5 Å of the adenylate carbonyl group.

RESULTS

Rationale for Selection of Residues for Mutagenesis. To examine the possibility that Luc undergoes a conformational change to catalyze the oxidative steps of light production, we used molecular-modeling techniques, described in the Materials and Methods, to first add LH_2-AMP to the putative active site (*29*, *33*) of the Luc crystal structure (*35*) and then to transform it into the bAcs conformation (*38*). An examination of the new model (Figures 4 and 5) showed that the Luc β-hairpin motif (^{442}IleLysTyrLysGlyTyrGln-Val^{449}) of region A8 was proximal to the active site and that Lys443 might make interactions to the adenylate. We targeted Lys443 along with nearby Lys445, residues in the motif capable of making both electrostatic and hydrogen-bonding interactions, for mutagenesis studies. We also focused on Gly446, an earlier recognized (*34*) stringently conserved superfamily residue that interacts with the 4′-phosphopantetheinyl group of CoA in the bAcs structure (*38*). Additionally, Gln448, the residue in an equivalent sequence position to Arg526, which in bAcs makes interactions with the phosphate of the analogue adenylate, the aromatic ring of CoA, and an N domain absolutely conserved glutamate, was mutated. In unpublished previous work, we had deter-

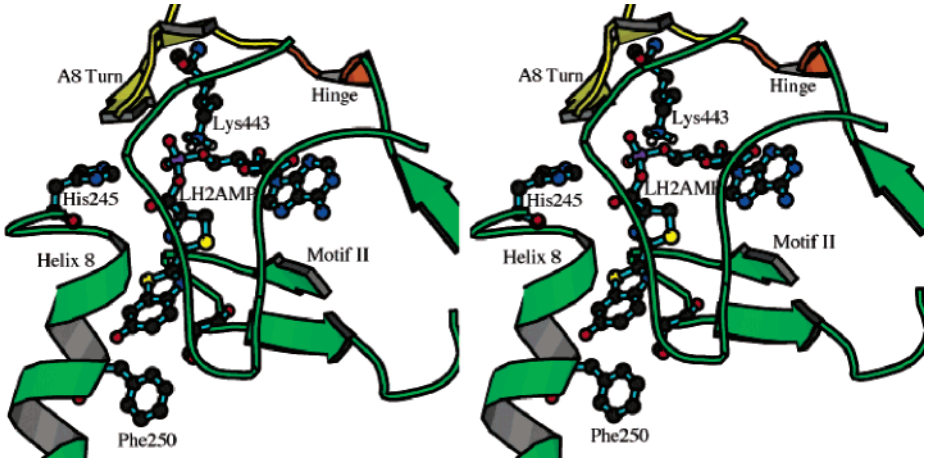

FIGURE 5: Putative active-site interactions of LH_2-AMP in Luc modeled into the bAcs conformation shown in Figure 4. The stereorepresentation shows LH_2-AMP and Lys443 in ball-and-stick models along with His245, Phe250, and Ser347 (unlabeled). Helix 8 (residues 246−258), a coil containing residues 301−321 (unlabeled), residues 340−358 that include motif II (residues 340−344), and residues 432−436 (unlabeled) extending to the hinge region are shown in green. The hinge (residues 437−439) is in orange, and residues 440−451, which include the A8 β hairpin (residues 442−449), are in yellow. This figure was produced with MolScript (*54*), BobScript (*55*), and POVScript+ (*56*).

Table 1: Steady-State Kinetic Constants for Overall Bioluminescence Reactions of Luciferase Enzymes at pH 7.8

enzyme	k_{cat} (s^{-1})[b]	K_m (μM)[a]		bioluminescence emission maximum (nm)[c]
		LH_2	Mg-ATP	
Ppy WT	1.67×10^{-1}	15.0	160.0	558 (62)
K443A	6.29×10^{-5}	2.3	48.6	558 (78)
K445Q	2.40×10^{-1}	8.9	69.0	556 (68)
G446I	2.00×10^{-2}	6.0	73.0	554 (63)
Q448A	8.75×10^{-2}	6.0	341.0	557 (70)
K529A	2.50×10^{-4}	230.0	1200.0	562 (93)
K443A/K529A	1.57×10^{-7}	67.0	560.0	596 (98)

[a] The error associated with the K_m value is within ±10% of the value. [b] k_{cat} values were obtained by dividing the V_{max} values (in units of Einstein $\times 10^{-6}$ s^{-1}) obtained from the measurements of K_m values for LH_2 by the amounts (in micromoles) of each luciferase used in each experiment. [c] Bioluminescence emission spectra were measured at pH 7.8 as described in the Materials and Methods, and bandwidths (nm) at 50% of emission maxima are indicated in parentheses.

mined that replacement of Tyr444 and Tyr447 with Phe produced little effect on the overall rate of bioluminescence.

Expression, Purification, and Preliminary Characterization of the Luciferase Proteins. The Ppy WT and modified luciferases listed in Table 1 were expressed as glutathione-*S*-transferase (GST)-fusion proteins and contained the additional N-terminal peptide GlyProLeuGlySer, which remained after PreScission protease cleavage from GST. Average yields (in milligrams) of purified proteins per 0.5 L of culture were Ppy WT (8.0), K443A (7.4), K445Q (8.6), G446I (3.2), Q448A (9.0), and K443A/K529A (13.0). Bioluminescence emission spectra produced by the K445Q, G446I, and Q448A luciferases at pH 7.8 with the natural substrates revealed no significant changes in bioluminescence color compared to Ppy WT (Table 1). The emission spectra of K443A and K529A, however, showed moderate to significant broadening, while the double mutant K443A/K529A produced a very broad somewhat red-shifted spectrum (Figure 3). These changes in the emission characteristics may indicate differences in the ability of the mutants to maintain the optimal environment of the emitter site.

Steady-State Kinetic Constants. The k_{cat} values in Table 1 relate the maximum achievable overall reaction rates for the combined adenylation and oxidation steps (eqs 1 and 2). We had previously studied (*31*) the single-site mutant K529A and a re-examination of its kinetic properties produced similar results, including the ~700-fold lower overall k_{cat} compared to Ppy WT (Table 1). A substantial ~2700-fold lower overall activity was obtained with the K443A enzyme; while the k_{cat} value of the double mutant K443A/K529A was reduced more than 1 000 000-fold. Interestingly, the K445Q mutant had a moderately 1.4-fold higher k_{cat} value.

Eliminating the side-chain group of Lys529 caused significantly increased K_m values of the K529A luciferase for both LH_2 (15-fold) and Mg-ATP (7.5-fold). In contrast, K443A had notably decreased K_m values for the natural substrates (6.5-fold for LH_2 and 3.3-fold for Mg-ATP). In the double mutant K443A/K529A, the K_m values for LH_2 and Mg-ATP increased 4.5- and 3.5-fold, respectively, increases less than those observed for K529A. With the exception of the ~2-fold increase in the Q448A K_m for Mg-ATP, the other single-point mutants had approximately 2 times lower K_m values for both substrates (Table 1).

Table 2: Apparent Kinetic Properties of Luciferase Enzymes with Synthetic LH_2-AMP at pH 7.8

enzyme	k_{cat} (s^{-1})[a]	K_m (μM)	k_{cat}/K_m (mM^{-1} s^{-1})	rise time (s)	decay time (min)[b]
Ppy WT	2.30×10^{-1}	4.7	48.9	0.4	0.04
K443A	1.01×10^{-4}	0.38	0.27	1.9	2.2
K445Q	3.20×10^{-1}	3.9	82.0	0.4	0.04
G446I	2.10×10^{-2}	1.5	9.5	1.3	0.23
Q448A	9.50×10^{-2}	2.2	43.2	0.8	0.10
K529A	1.75×10^{-1}	12.6	13.9	0.5	0.12
K443A/K529A	3.11×10^{-5}	0.55	0.057	3.6	3.5

[a] Kinetic constants were determined with synthetic LH_2-AMP as described in the Materials and Methods. The error associated with K_m and k_{cat} falls within ±10% of the value. [b] Bioluminescence decay times (to 20% of initial activity) were measured from maximum initial flash heights.

Effects of Luciferase Mutations on the Luc Adenylation and Oxidation Partial Reactions. Measurements of the kinetic properties of Ppy WT and the Luc mutants with synthetic LH_2-AMP as the sole substrate were undertaken to evaluate the effects of the amino acid changes on the Luc-catalyzed oxidative chemistry (eq 2) subsequent to and independent of the rate of adenylate formation (eq 1). With the synthetic adenylate, the luciferase mutants K443A and K443A/K529A had significantly reduced k_{cat} values (2300- and 7400-fold, respectively) and prolonged light emission profiles (rise and decay times) compared to Ppy WT (Table 2). Extended rise and decay times of the oxidative partial reaction may indicate reduced rates of both C-4 anion formation and product inhibition. As previously reported (*31*), the K529A mutant behaved similarly to Ppy WT with the adenylate (Table 2). The K_m value (4.7 μM) of Ppy WT for LH_2-AMP was ~3-fold lower than the K_m for LH_2. Similar K_m values were obtained for the Luc mutants with the exception of K443A and K443A/K529A, which had significantly lower K_m values for the adenylate of 0.38 and 0.55 μM, respectively.

Measurements of the enzyme-catalyzed rates of formation of the adenylate of synthetic dehydroluciferin (L-AMP) were used to approximate (*31*) the rates of formation of LH_2-AMP in Ppy WT and the mutant luciferases. The decrease in fluorescence at 440 nm (excitation at 350 nm) was recorded over time for solutions of luciferases, L, and Mg-ATP, and the data were analyzed as described previously (*31*). The estimated rates for the adenylation partial reaction are presented in Table 3. Near normal rates of adenylate formation were observed for the K443A, K445Q, G446I, and Q448A mutants. However, K529A and the double mutant K443A/K529A exhibited 100-fold slower rates of adenylation.

Effect of CoA on Total Light Output. The addition of CoA to a bioluminescence reaction of Ppy WT caused an approximate doubling of the total light emission (Table 3). This increase in light output is a result of sustained light emission associated with a slower decay of bioluminescence and not an increase in the maximum bioluminescence intensity (data not shown). A similar result was observed with Q448A, while an increase of only 34% was observed with the K445Q luciferase. Notably, G446I and K443A were completely insensitive to the enhancing effect of CoA.

Table 3: Estimated Relative Rates of Partial Reactions and CoA Effect on Total Bioluminescence of Luciferase Enzymes at pH 7.8

enzyme	overall rate[a]	adenylation rate[b]	oxidative rate[c]	effect of CoA on overall light yield[d]
Ppy WT	100.0	100.0	100.0	1.9
K443A	0.038	100.0	0.044	1.0
K445Q	143.7	80.0	139.1	1.3
G446I	12.0	91.0	9.3	1.0
Q448A	52.4	98.0	41.3	2.0
K529A	0.150	1.0	76.1	nd
K443A/K529A	9.40×10^{-5}	1.0	0.014	nd

[a] Relative overall rates are based on overall k_{cat} values (Table 1) with substrates LH_2 and Mg-ATP. [b] Relative rates of adenylation are based on k_{cat} values for enzyme-catalyzed measurements of L-AMP formation from L and Mg-ATP as described under the Materials and Methods. [c] Relative oxidative rates are based on k_{cat} values for reactions using synthetic LH_2-AMP as a substrate (Table 2). [d] The effect of 0.1 mM CoA on light production was determined for Ppy WT and mutant luciferase enzymes as described in the Materials and Methods. The values reflect the effect of CoA on bioluminescence reactions performed in the presence of 0.1 mM CoA and are expressed relative to values obtained in identical studies performed with the same enzyme but in the absence of CoA. Values for K529A and K443A/K529A were not determined (nd) because of the especially prolonged decay times of 100 and 120 min, respectively.

DISCUSSION

Mutagenesis Evidence that the Luc Partial Reactions are Catalyzed by Two Conformations. This investigation was stimulated by the disclosure of the bAcs crystal structure and the accompanying proposal by Gulick et al. (*38*) that the superfamily of adenylate-forming enzymes catalyze two partial reactions (Figure 1) by adopting the two different conformations illustrated by PheA and bAcs (Figure 2). Evidence cited (*38*) in support of this hypothesis included the observation that bAcs, PheA, and DhbE have a very similar secondary structure with only moderate sequence homology, yet they catalyze very similar sequential reactions. These enzymes and yAcs have two highly conserved motifs, A8 (Asp436-Glu455 in Luc) and A10 (Thr527-Arg533 in Luc), which are on opposite sides of their C domains, ~30 Å away from each other. In the PheA conformation, Lys517 (Lys529 in Luc) of A10 is at the active site interacting with substrate Phe and AMP; similar interactions are observed between the equivalent DhbE residue and its substrates and adenylate (*37*). In contrast, in bAcs, the equivalent residue Lys609 is located ~27 Å from the active-site-bound alkyl-AMP inhibitor. Mutation of the residue equivalent to Lys609 in a related propionyl-CoA synthetase substantially reduced the rate of the adenylation partial reaction without reducing the rate of the second half-reaction (*25*). In the bAcs conformation, motif A8 residue Arg526 (Gln448 in Luc) interacts with a phosphate oxygen of the inhibitor, forming a salt bridge with Glu417 (Glu344 in Luc). While we were unable to find an example of conclusive evidence for the participation of a motif A8 β-hairpin residue exclusively in the second partial reaction, we note the report of Stuible et al. (*20*) that point mutations to Lys445 (Lys443 in Luc) and Lys457 (Lys445 in Luc) in 4-coumarate:CoA ligase At4CL2 reduced the overall rate of production of caffeoyl-CoA by 96−99%. This result is suggestive that the A8 β-hairpin motif is important for efficient CoA displacement of AMP and that this motif is repositioned by rotation from the PheA conformation into that of bAcs.

Luc shares remarkable domain and secondary-structural similarity with the PheA, DhbE, bAcs, and yAcs structures. Although the open conformation of the Luc crystal structure (Figure 2) is unlike those of the PheA group or bAcs, we believe that Luc assumes the PheA conformation in the presence of substrates and that efficient LH_2-AMP formation requires the A10 motif residue Lys529 as demonstrated previously (*31*) and in this work (Tables 1−3). Lys529 has little effect on the second partial reaction, the oxidation of the adenylate (Tables 2 and 3). The adenylation half-reactions catalyzed by the superfamily enzymes very likely all proceed in the PheA conformation.

The second half-reactions of the superfamily enzymes, typified by the CoA thiol displacement of AMP, are quite similar with the apparent exception of the multistep oxidation of LH_2-AMP catalyzed by the luciferases (Figure 1). The results of our systematic mutagenesis study of the A8 β-hairpin motif of Luc (Tables 2 and 3) provide convincing evidence that Lys443 is critical for efficient catalysis of only the oxidative chemistry, while the other motif residues have little effect on the utilization of LH_2-AMP. We have demonstrated that in Luc, two Lys residues ~30 Å apart on opposite sides of the C domain and absolutely conserved in all luciferases are each essential for one and only one of the partial reactions of firefly bioluminescence. We believe that these experimental findings are best explained by the domain rotation hypothesis of Gulick et al. (*38*) and that Lys529 promotes LH_2-AMP formation, while Lys443 promotes its oxidation in conformations similar to those of PheA and bAcs, respectively.

Role of the A8 β-Hairpin Motif in CoA Binding. In the bAcs crystal structure (*38*), CoA is mainly bound to the surface of the enzyme. The amino NH groups of the pantetheinyl moiety form a distorted β-sheet with the main-chain carbonyl groups of A8 residues Ser523 (Lys445 in Luc) and Gly524 (Gly446 in Luc) that orients the terminal thiol toward the C1 carbon of the propyl group of the adenylate analogue. A similar conformation with acetyl-AMP present would be expected to promote the second partial reaction that requires the thiol to attack the carbonyl group of the acyl-adenylate. This step does not occur in Luc, and CoA is not required for the oxidative reaction that produces light in the firefly. However, McElroy and DeLuca had long ago recognized (*49*) that the ability of Luc to use CoA to synthesize L-SCoA from L-AMP was similar to fatty acid activation by acyl-CoA synthetases (eq 3). The formation of the potent Luc inhibitor L-AMP that accompanies *in vitro* bioluminescence very likely accounts for the characteristic rapid decay of light emission *(28, 50)*. Because it lacks a C-4 proton, L-AMP cannot be oxidized by Luc. The sustenance of bioluminescence by addition of CoA can double the total light output of Ppy WT because the production of L-SCoA is accompanied by the release of free Luc (*26, 28*). Our findings that mutations to Lys443, Lys445, and Gly446 diminish or abolish the enhancing effect of CoA on bioluminescence (Table 3) likely result from disruptions of binding interactions, similar to those observed in the bAcs structure (*38*), between the A8 β-hairpin motif and the pantetheinyl group of CoA. Moreover, the poor CoA enhancement of the K445A enzyme, which is an excellent

light producer, suggests that the reduced overall activity resulting from mutation of the equivalent residue (Lys457) of the 4-coumarate:CoA ligase At4CL2 (*20*) resulted mainly from disrupted CoA binding affecting only the second partial reaction.

$$\text{Luc} + \text{L} + \text{ATP} \overset{Mg^{2+}}{\rightleftharpoons} \text{Luc}\cdot\text{L-AMP} \xrightarrow{\text{CoASH}} \text{Luc} + \text{L-SCoA} + \text{AMP} \quad (3)$$

Gulick et al. have suggested (*38*) that CoA is required to adopt the bAcs-rotated conformation. This may be the case for the CoA-requiring adenylate-forming enzymes; however, it is also possible that the PheA and bAcs conformations are both readily populated in solution in the absence of CoA. The bAcs crystal containing an adenylate analogue that cannot react further could represent the rotated conformation trapped by CoA. In this study, we have provided evidence that mutations of residues in the distant A8 and A10 motifs both affect the binding of Luc substrates LH_2, Mg-ATP, and LH_2-AMP (Tables 1 and 2). These results provide further support for our contention that Luc (and perhaps the other superfamily proteins) exists in both the PheA and bAcs conformations (and possibly others) in solution and that it catalyzes one half-reaction from each of the two conformations observed so far.

Role of Lys443 in Luc Catalysis. Using the k_{cat} and K_m data obtained with LH_2-AMP as the only added substrate (Table 2), we examined the effects of the single and double mutations Lys443Ala and Lys529Ala on transition-state stabilization of the second half-reaction of Luc catalysis. Changes in the transition-state stabilization ($\Delta\Delta G^{\ddagger}$) introduced by the single and double mutations were estimated (data not shown) from the k_{cat} and k_{cat}/K_m data for the K443A, K529A, and K443A/K529A enzymes (*51*). Analyses of both the k_{cat} and k_{cat}/K_m data using the method described by Mildvan et al. (*52*) revealed that the combined effects of the free energy changes of the single Lys mutations were additive. While this result may be interpreted in several ways (*52*), it is consistent with the notion that Lys443 and Lys529 function independently in consecutive steps, one of which is rate-determining. The rate-determining step in firefly bioluminescence (*53*) is the Luc-assisted abstraction of the C-4 proton of LH_2-AMP (step b of Figure 1). A model for bioluminescent reactions initiated by the addition of preformed LH_2-AMP to Luc that is consistent with the additive nature of the Lys mutations is that the oxidative partial reaction (eq 2) involves two consecutive steps: (1) the formation of the Luc·LH_2-AMP complex aided by Lys529, followed by (2) the Lys443-dependent generation of a Luc complex of an intermediate resembling the substrate undergoing proton abstraction (Figure 6). The kinetic data for the K443A mutant suggest that Lys443 contributes significantly to catalysis but that it is not the sole essential residue. Among several possibilities, we favor a role for Lys443 like that depicted in Figure 6, which is intended to illustrate that the Lys residue participates in the rate-determining step by stabilizing the developing negative charge accompanying proton abstraction. A similar process, illustrated with CoA in Figure 6, could account for the catalytic role of the equivalent Lys residue in the 4-coumarate:CoA ligases and NRPSs. Possibly too, Arg526 in bAcs has a similar role in assisting thioester formation. Alternatively, the proximity of the Arg526 (or Lys443 of Luc) side chains could promote AMP release necessary for thioester (or dioxetanone) formation (step d of Figure 1). These speculative catalytic roles of the basic residues of the A8 β-hairpin domain suggest a common catalytic theme for the diverse second partial reactions of the entire superfamily of acyl-adenylate-forming enzymes, including the luciferases.

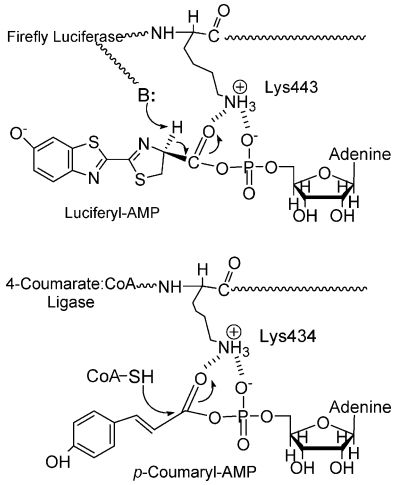

FIGURE 6: Hypothetical stabilization of the developing negative charge in the second half-reactions catalyzed by the firefly luciferases and 4-coumarate:CoA ligases.

ACKNOWLEDGMENT

We thank Susan Gonzalez, Sarah Fleet, and Evelyn Bamford for technical assistance.

REFERENCES

1. White, E. H., Rapaport, E., Seliger, H. H., and Hopkins, T. A. (1971) The chemi- and bioluminescence of firefly luciferin: An efficient chemical production of electronically excited states, *Bioorg. Chem. 1*, 92−122.
2. DeLuca, M. (1976) Firefly luciferase, *Adv. Enzymol. 44*, 37−68.
3. Wood, K. V. (1995) The chemical mechanism and evolutionary development of beetle bioluminescence, *Photochem. Photobiol. 62*, 662−673.
4. Hastings, J. W. (1995) Bioluminescence, in *Cell Physiology Source Book* (Sperelakis, N., Ed.) pp 665−681, Academic Press, New York.
5. Koo, J.-Y., Schmidt, S. P., and Schuster, G. B. (1978) Bioluminescence of the firefly: Key steps in the formation of the electronically excited state for model systems, *Proc. Natl. Acad. Sci. U.S.A. 75*, 30−33.
6. Seliger, H. H., and McElroy, W. D. (1960) Spectral emission and quantum yield of firefly bioluminescence, *Arch. Biochem. Biophys. 88*, 136−141.
7. Wood, K. V., Lam, Y. A., Seliger, H. H., and McElroy, W. D. (1989) Complementary DNA coding click beetle luciferases can elicit bioluminescence of different colors, *Science 244*, 700−702.
8. Ohmiya, Y., Ohba, N., Toh, H., and Tsuji, F. I. (1995) Cloning, expression, and sequence analysis of cDNA for the luciferases from the Japanese fireflies, *Pyrocoelia miyako* and *Hotaria parvula*, *Photochem. Photobiol. 62*, 309−313.
9. Gruber, M. K., Kutuzova, G. D., and Wood, K. V. (1996) Cloning and expression of a *Phengodes* luciferase, in *Bioluminescence and Chemiluminescence: Molecular Reporting with Photons* (Hastings, J. W., Kricka, L. J., and Stanley, P. E., Eds.) pp 244−247, John Wiley and Sons, Chichester, U.K.

10. Ye, L., Buck, L. M., Schaeffer, H. J., and Leach, F. R. (1997) Cloning and sequencing of a cDNA for firefly luciferase from *Photuris pennsylvanica*, *Biochim. Biophys. Acta 1339*, 39−52.
11. Viviani, V. R., Bechara, E. J. H., and Ohmiya, Y. (1999) Cloning, sequence analysis, and expression of active *Phrixothrix* railroad worms luciferases: Relationship between bioluminescence spectra and primary structures, *Biochemistry 38*, 8271−8279.
12. Viviani, V. R., Silva, A. C. R., Perez, G. L. O., Santelli, R. V., Bechara, E. J. H., and Reinach, F. C. (1999) Cloning and molecular characterization of the cDNA for the Brazilian larval click-beetle *Pyrearinus termitilluminans* luciferase, *Photochem. Photobiol. 70*, 254−260.
13. Lee, K. S., Park, H. J., Bae, J. S., Goo, T. W., Kim, I., Sohn, H. D., and Jin, B. R. (2001) Molecular cloning and expression of a cDNA encoding the luciferase from the firefly, *Pyrocoelia rufa*, *J. Biotechnol. 92*, 9−19.
14. Choi, Y. S., Lee, K. S., Bae, J. S., Lee, K. M., Kim, S. R., Kim, I., Lee, S. M., Sohn, H. D., and Jin, B. R. (2002) Molecular cloning and expression of a cDNA encoding the luciferase from the firefly, *Hotaria unmunsana*, *Comp. Biochem. Physiol., Part B: Biochem. Mol. Biol. 132*, 661−670.
15. Suzuki, H., Kawarabayasi, Y., Kondo, J., Abe, T., Nishikawa, K., Kimura, S., Hashimoto, T., and Yamamoto, T. (1990) Structure and regulation of rat long-chain acyl-CoA synthetase, *J. Biol. Chem. 265*, 8681−8685.
16. Babbitt, P. C., Kenyon, G. L., Martin, B. M., Charest, H., Sylvestre, M., Scholten, J. D., Chang, K.-H., Liang, P.-H., and Dunaway-Mariano, D. (1992) Ancestry of the 4-chlorobenzoate dehalogenase: Analysis of amino acid sequence identities among families of acyl:adenyl ligases, enoyl-CoA hydratases/isomerases, and acyl-CoA thioesterases, *Biochemistry 31*, 5594−5604.
17. Chang, K.-H., Xiang, H., and Dunaway-Mariano, D. (1997) Acyl-adenylate motif of the acyl-adenylate/thioester-forming enzyme superfamily: A site-directed mutagenesis study with the *Pseudomonas* sp. strain CBS3 4-chlorobenzoate:CoA ligase, *Biochemistry 36*, 15650−15659.
18. Watkins, P. A. (1997) Fatty acid oxidation, *Prog. Lipid Res. 36*, 55−83.
19. An, J. H., Lee, G. Y., Jung, J. W., Lee, W., and Kim, Y. S. (1999) Identification of residues essential for a two-step reaction by malonyl-CoA synthetase from *Rhizobium trifolii*, *Biochem. J. 344*, 159−166.
20. Stuible, H. P., Buttner, D., Ehlting, J., Hahlbrock, K., and Kombrink, E. (2000) Mutational analysis of 4-coumarate:CoA ligase identifies functionally important amino acids and verifies its close relationship to other adenylate-forming enzymes, *FEBS Lett. 467*, 117−122.
21. Kleinkauf, H., and von Doehren, H. (1996) A nonribosomal system of peptide biosynthesis, *Eur. J. Biochem. 236*, 335−351.
22. Dieckmann, R., Pavela-Vrancic, M., Pfeifer, E., von Döhren, H., and Kleinkauf, H. (1997) The adenylation domain of tyrocidine synthetase 1. Structural and functional role of the interdomain linker region and the (S/T)GT(T/S)GXPKG core sequence, *Eur. J. Biochem. 247*, 1074−1082.
23. Marahiel, M. A., Stachelhaus, T., and Mootz, H. D. (1997) Modular peptide synthetases involved in nonribosomal peptide synthesis, *Chem. Rev. 97*, 2651−2673.
24. Keating, T. A., and Walsh, C. T. (1999) Initiation, elongation, and termination strategies in polyketide and polypeptide antibiotic biosynthesis, *Curr. Opin. Chem. Biol. 3*, 598−606.
25. Horswill, A. R., and Escalante-Semerena, J. C. (2002) Characterization of the propionyl-CoA synthetase (PrpE) enzyme of *Salmonella enterica*: Residue Lys592 is required for propionyl-AMP synthesis, *Biochemistry 41*, 2379−2387.
26. Airth, R. L., Rhodes, W. C., and McElroy, W. D. (1958) The function of coenzyme A in luminescence, *Biochim. Biophys. Acta 27*, 519−532.
27. Pazzagli, M., Devine, J. H., Peterson, D. O., and Baldwin, T. O. (1992) Use of bacterial and firefly luciferases as reporter genes in DEAE-dextran-mediated transfection of mammalian cells, *Anal. Biochem. 204*, 315−323.
28. Fraga, H., Esteves da Silva, J. C. G., and Fontes, R. (2004) Chemical synthesis and firefly luciferase produced dehydroluciferyl-coenzyme A, *Tetrahedron Lett. 45*, 2117−2120.
29. Branchini, B. R., Magyar, R. A., Murtiashaw, M. H., Anderson, S. M., and Zimmer, M. (1998) Site-directed mutagenesis of histidine 245 in firefly luciferase: A proposed model of the active site, *Biochemistry 37*, 15311−15319.
30. Branchini, B. R., Magyar, R. A., Murtiashaw, M. H., Anderson, S. M., Helgerson, L. C., and Zimmer, M. (1999) Site-directed mutagenesis of firefly luciferase active site amino acids: A proposed model for bioluminescence color, *Biochemistry 38*, 13223−13230.
31. Branchini, B. R., Murtiashaw, M. H., Magyar, R. A., and Anderson, S. M. (2000) The role of lysine 529, a conserved residue of the acyl-adenylate-forming enzyme superfamily, in firefly luciferase, *Biochemistry 39*, 5433−5440.
32. Branchini, B. R., Magyar, R. A., Murtiashaw, M. H., and Portier, N. C. (2001) The role of active site residue arginine 218 in firefly luciferase bioluminescence, *Biochemistry 40*, 2410−2418.
33. Branchini, B. R., Southworth, T. L., Murtiashaw, M. H., Boije, H., and Fleet, S. E. (2003) A mutagenesis study of the putative luciferin binding site residues of firefly luciferase, *Biochemistry 42*, 10429−10436.
34. Conti, E., Franks, N. P., and Brick, P. (1996) Crystal structure of firefly luciferase throws light on a superfamily of adenylate-forming enzymes, *Structure 4*, 287−298.
35. Franks, N. P., Jenkins, A., Conti, E., Lieb, W. R., and Brick, P. (1998) Structural basis for the inhibition of firefly luciferase by a general anesthetic, *Biophys. J. 75*, 2205−2211.
36. Conti, E., Stachelhaus, T., Marahiel, M. A., and Brick, P. (1997) Structural basis for the activation of phenylalanine in the nonribosomal biosynthesis of gramicidin S, *EMBO J. 16*, 4174−4183.
37. May, J. J., Kessler, N., Marahiel, M. A., and Stubbs, M. T. (2002) Crystal structure of DhbE, an archetype for aryl acid activating domains of modular nonribosomal peptide synthetases, *Proc. Natl. Acad. Sci. U.S.A. 99*, 12120−12125.
38. Gulick, A. M., Starai, V. J., Horswill, A. R., Homick, K. M., and Escalante-Semerena, J. C. (2003) The 1.75 Å crystal structure of acetyl-CoA synthetase bound to adenosine-5′-propylphosphate and coenzyme A, *Biochemistry 42*, 2866−2873.
39. Jogl, G., and Tong, L. (2004) Crystal structure of yeast acetyl-coenzyme A synthetase in complex with AMP, *Biochemistry 43*, 1425−1431.
40. Stachelhaus, T., Mootz, H. D., and Marahiel, M. A. (1999) The specificity-conferring code of adenylation domains in nonribosomal peptide synthetases, *Chem. Biol. 6*, 493−505.
41. Branchini, B. R., Murtiashaw, M. H., Magyar, R. A., Portier, N. C., Ruggiero, M. C., and Stroh, J. G. (2002) Yellow-green and red firefly bioluminescence from 5,5-dimethyloxyluciferin, *J. Am. Chem. Soc. 124*, 2112−2113.
42. Altschul, S. F., Madden, T. L., Schaffer, A. A., Zhang, J. H., Zhang, Z., Miller, W., and Lipman, D. J. (1997) Gapped BLAST and PSI-BLAST: A new generation of protein database search programs, *Nucleic Acids Res. 25*, 3389−3402.
43. Pollastri, G., Przybylski, D., Rost, B., and Baldi, P. (2002) Improving the prediction of protein secondary structure in three and eight classes using recurrent neural networks and profiles, *Proteins: Struct., Funct., Genet. 47*, 228−235.
44. Guarnieri, F., and Still, W. C. (1994) A rapidly convergent simulation method: Mixed Monte Carlo/stochastic dynamics, *J. Comput. Chem. 15*, 1302−1310.
45. Senderowitz, H., Guarnieri, F., and Still, W. (1995) A smart Monte Carlo technique for free energy simulations of multiconformational molecules. Direct calculations of the conformational populations of organic molecules, *J. Am. Chem. Soc. 117*, 8211−8219.
46. Keseru, G. M., and Kolossvary, I. (2001) Fully flexible low-mode docking: Application to induced fit in HIV integrase, *J. Am. Chem. Soc. 123*, 12708−12709.
47. Kolossvary, I., and Keseru, G. M. (2001) Hessian-free low-mode conformational search for large-scale protein loop optimization: Application to c-jun N-terminal kinase JNK3, *J. Comput. Chem. 22*, 21−30.
48. Qiu, D., Shenkin, P., Hollinger, F., and Still, W. C. (1997) The GB/SA continuum model for solvation. A fast analytical method for the calculation of approximate born radii, *J. Phys. Chem. 101*, 3005.
49. McElroy, W. D., DeLuca, M., and Travis, J. (1967) Molecular uniformity in biological catalyses. The enzymes concerned with firefly luciferin, amino acid, and fatty acid utilization are compared, *Science 157*, 150−160.
50. Rhodes, W. C., and McElroy, W. D. (1958) The synthesis and function of luciferyl-adenylate and oxyluciferyl-adenylate, *J. Biol. Chem. 233*, 1528−1537.

51. Wilkinson, A. J., Fersht, A. R., Blow, D. M., and Winter, G. (1983) Site-directed mutagenesis as a probe of enzyme structure and catalysis: Tyrosyl-tRNA synthetase cysteine-35 to glycine-35 mutation, *Biochemistry 22*, 3581−3586.
52. Kuliopulos, A., Talalay, P., and Mildvan, A. S. (1990) Combined effects of two mutations of catalytic residues on the ketosteroid isomerase reaction, *Biochemistry 29*, 10271−10280.
53. McCapra, F., Gilfoyle, D. J., Young, D. W., Church, N. J., and Spencer, P. (1994) The chemical origin of colour differences in beetle bioluminescence, in *Bioluminescence and Chemiluminescence: Fundamentals and Applied Aspects* (Campbell, A. K., Kricka, L. J., and Stanley, P. E., Eds.) pp 387−391, John Wiley and Sons, Chichester, U.K.
54. Kraulis, P. J. (1991) MOLSCRIPT: A program to produce both detailed and schematic plots of protein structures, *J. Appl. Crystallogr. 24*, 946−950.
55. Esnouf, R. M. (1999) Further additions to MolScript version 1.4, including reading and contouring of electron-density maps, *Acta Crystallogr., Sect. D 55*, 938−940.
56. Fenn, T. D., Ringe, D., and Petsko, G. A. (2003) POVScript+: A program for model and data visualization using persistence of vision ray-tracing, *J. Appl. Crystallogr. 36*, 944−947.
57. Merritt, E. A., and Bacon, D. J. (1997) Raster3D: Photorealistic molecular graphics, *Methods Enzymol. 277*, 505−524.

BI047903F